J Biol Inorg Chem (2015) 20:447–460
DOI 10.1007/s00775-014-1230-6

MINIREVIEW

The discovery of Mo(III) in FeMoco: reuniting enzyme and model chemistry

Ragnar Bjornsson · Frank Neese · Richard R. Schrock · Oliver Einsle · Serena DeBeer

Received: 31 August 2014 / Accepted: 11 December 2014 / Published online: 31 December 2014

Abstract Biological nitrogen fixation is enabled by molybdenum-dependent nitrogenase enzymes, which effect the reduction of dinitrogen to ammonia using an Fe_7MoS_9C active site, referred to as the iron molybdenum cofactor or FeMoco. In this mini-review, we summarize the current understanding of the molecular and electronic structure of FeMoco. The advances in our understanding of the active site structure are placed in context with the parallel evolution of synthetic model studies. The recent discovery of Mo(III) in the FeMoco active site is highlighted with an emphasis placed on the important role that model studies have played in this finding. In addition, the reactivities of synthetic models are discussed in terms of their relevance to the enzymatic system.

Responsible Editors: José Moura and Paul Bernhardt.

R. Bjornsson · F. Neese · S. DeBeer (✉)
Max-Planck-Institut für Chemische Energiekonversion, Stiftstr. 34-36, 45470 Mülheim and Der Ruhr, Germany
e-mail: serena.debeer@cec.mpg.de

R. Bjornsson (✉)
Science Institute, University of Iceland, Dunhagi 3, IS-107 Reykjavik, Iceland
e-mail: ragnarbj@hi.is

R. R. Schrock
Department of Chemistry 6-331, Massachusetts Institute of Technology, 77 Massachusetts Avenue, 6-331, Cambridge, MA 02139, USA

O. Einsle
Institute for Biochemistry, Albert-Ludwigs-Universität Freiburg, Albertstrasse 21, 79104 Freiburg, Germany

S. DeBeer
Department of Chemistry and Chemical Biology, Cornell University, Ithaca, NY 14853, USA

Keywords Nitrogenase · FeMoco · Molybdenum · Model compounds · Catalysis

Introduction

Molybdenum-dependent nitrogenase is a complex enzyme that catalyzes the formation of ammonia through the electrochemical reduction of dinitrogen at ambient temperature and pressure, utilizing eight electrons, eight protons and 16 MgATP molecules [1, 2]. Unraveling the structural and mechanistic details of how nature activates the strong bond of dinitrogen is of fundamental importance, potentially aiding in catalyst design.

The molybdenum–iron component (MoFe) of nitrogenase has two types of complex metal clusters, the "P-cluster" and the FeMo cofactor (FeMoco) (Fig. 1). The P-cluster is an eight-iron cluster that appears to serve as an electron-transfer site, while FeMoco is generally agreed to be the site of dinitrogen reduction. The FeMo cofactor consists of 7 irons, 1 molybdenum, 9 sulfides and an interstitial light atom that was recently identified as carbon by XES, ESEEM and high-resolution crystallography [3, 4].

FeMoco has fascinated chemists for decades. This complex cofactor, whose structural details have been elusive for so long, is capable of chemistry that is still a challenge for synthetic chemists to mimic. While the molecular structure details of FeMoco are finally clear, many uncertainties remain about the $S = 3/2$ resting form (the dithionite-isolated form, also called E_0) of the enzyme. The total charge of the cofactor, the metal oxidation states and the electronic structure, all remain open questions—the answers to which are essential for any informed discussion of the molecular level mechanism of dinitrogen reduction.

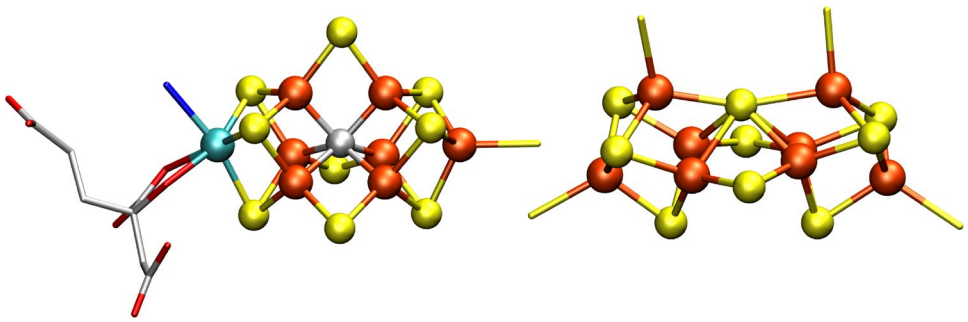

Fig. 1 The metal clusters of nitrogenase MoFe protein: FeMoco and P-cluster

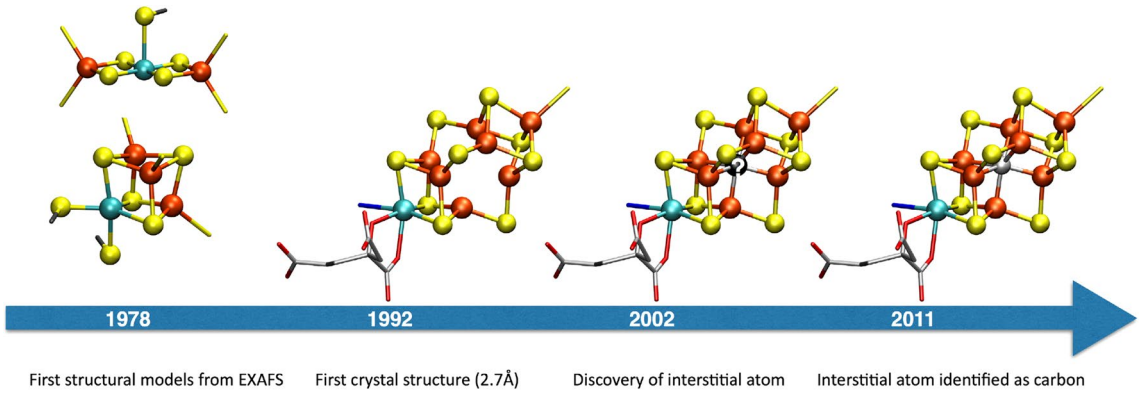

Fig. 2 Evolution of FeMoco structures. From the first EXAFS-proposed structures to the current 2011 structure

In this mini-review, we give a brief overview of the structural characterization of the enigmatic FeMoco cluster, including both molecular and electronic structure aspects. The evolution of our structural understanding of FeMoco is complemented by a review of FeMoco-inspired synthetic model chemistry. The strong synergy between model chemistry and the advances in our understanding of FeMoco active site structure are highlighted. Furthermore, the reactivity of the model complexes is discussed in terms of its potential relevance to the enzyme chemistry.

First structural models

Prior to the first crystal structure of MoFe protein, structural modeling of FeMoco (as well as the P-cluster) relied primarily on information from X-ray absorption spectroscopy (XAS) with a focus on the extended X-ray absorption fine structure (EXAFS) region to acquire basic molecular structural information. In 1978, Hodgson and coworkers [5] published the first structural models based on EXAFS data from Mo XAS experiments on MoFe protein (Fig. 2). The data indicated 3–4 sulfur atoms at a 2.36 Å distance from the molybdenum and 2–3 iron atoms at 2.72 Å. The models proposed, included a cubane-type structure and a linear Fe–Mo–Fe compound.

The initial EXAFS structural models for FeMoco served as inspiration for the synthetic Mo–Fe–S based chemistry that several research groups explored in detail for the next decades, particularly the groups of Holm [6] and Coucouvanis [7]. Holm and coworkers explored a self-assembly route to Mo–Fe–S clusters based on the observed spontaneous formation of Fe_4S_4 cubane clusters from simple reactants such as $FeCl_3$ and NaSH and NaSR. Adding $[MoS_4]^{2-}$ to the reaction mixture afforded the first Mo–Fe–S double cubanes, synthesized by the groups of Holm and Garner [8–12] in the period of 1978–1980. These compounds were the first heterometal weak field cubane clusters to be synthesized and sparked the beginning of nitrogenase-inspired model compound chemistry that continues to be explored today (Fig. 3).

As the EXAFS structural data on FeMoco suggested a single molybdenum atom per cluster (and a single cubane), single cubane Mo–Fe–S compounds were the next synthetic goal. Cleavage of double cubanes resulted in the first single $[MoFe_3S_4]$ cubanes reported between 1981 and 1983, which showed close similarity to the original single cubane FeMoco EXAFS proposal (Fig. 2) [13–15].

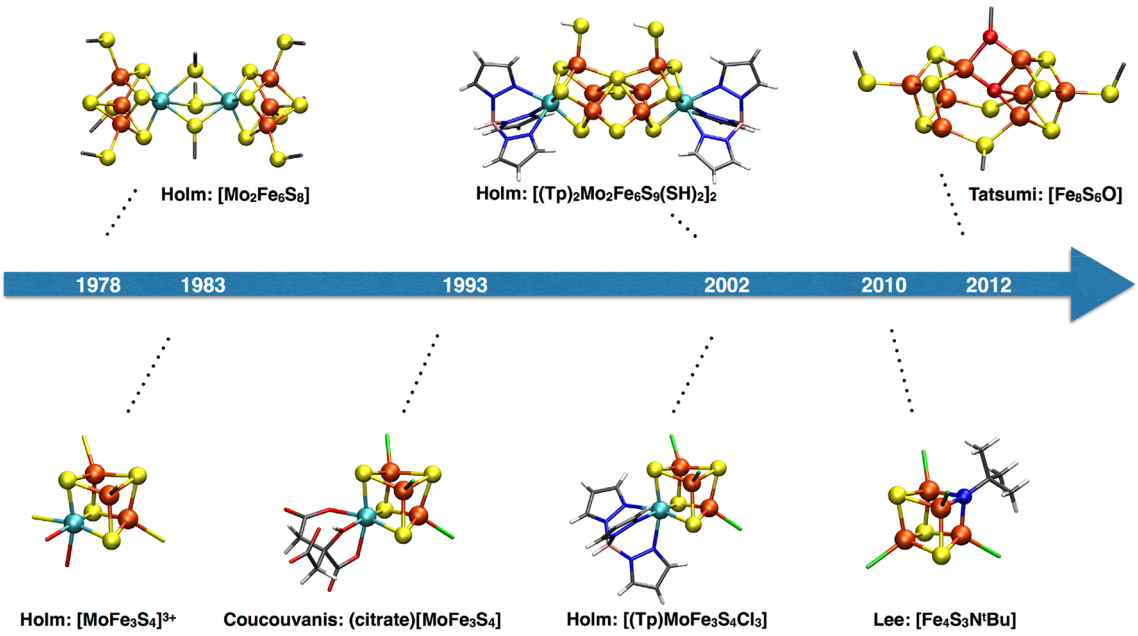

Fig. 3 Selected FeMoco-inspired model cubanes created in the period of 1978–2012

In 1982, however, Fe EXAFS data indicated second-shell Fe–Fe interactions [16], indicating that the cofactor was a larger cluster rather than a single cubane. The complexity of the FeMoco active site was confirmed in 1992, when the first crystal structure of MoFe protein became available from Rees et al. [17]. The 2.7 Å structure revealed a complicated $MoFe_7S_9$ structure that was neither a cubane nor a double cubane, as a corner atom of each cube appeared to be missing (see Fig. 2).

The structure had surprising features: six three-coordinate iron atoms and a vacant cavity, and it was the source of confusion for many years.

For example, ^{57}Fe Mössbauer studies of FeMoco were interpreted in view of the trigonal Fe ions that had no synthetic analogs, and both isomer shifts and quadrupole splittings were found to be unusual and puzzling [18, 19]. This finding, however, did inspire research focused on low-coordinate iron complexes as synthetic models of nitrogenase [20–23]. While the direct correlation to the resting form of nitrogenase no longer held upon discovery of the central atom, it is still speculated that 3-coordinate iron sites could have relevance to intermediates in the N_2 reduction process [23, 24].

In fact, it was proposed early on that the trigonal irons in nitrogenase would be highly reactive and likely to bind substrate (even within the cavity). Multiple reaction mechanisms were proposed from quantum chemical calculations [25–29]. The vacant cavity was even proposed to become occupied by a hydride upon reduction [30]. The structure also further inspired Mo–Fe–S cluster chemistry and new cubane clusters void of a corner sulfide were synthesized [31–33].

The confusing aspects of the FeMoco structure were not resolved until 2002 [34], when a more highly resolved structure revealed an interstitial light atom that could be assigned as either an oxygen, a nitrogen or a carbon. In 2011, the light atom was confidently demonstrated to be carbon by both Fe X-ray emission [4] and X-ray crystallography techniques [3] (see JBIC review by Einsle [35]). The discovery of the interstitial atom confirmed the structure of FeMoco to be cubane-like after all (a fused double cubane structure with four-coordinate distorted tetrahedral irons), which re-established the biological relevance of the synthetic single and double Mo–Fe–S cubanes.

The synthetic Mo–Fe–S cubane structures are highly reminiscent of half of the full FeMoco cluster (see Fig. 4), with the interstitial carbide in FeMoco taking the role of a corner sulfide. A comparison of Mo–Fe, Mo–S, Fe–Fe and Fe–S distances in one such $[MoFe_3S_4]^{3+}$ cluster ($[(Tp)MoFe_3S_4Cl_3]^{1-}$ from Ref. [36]) and the most recent 1.0 Å X-ray crystal structure of MoFe protein shows this to be true. The major structural difference between a $[MoFe_3S_4]$ cubane and the cubane-half of FeMoco is the carbide in FeMoco. The smaller carbide in FeMoco distorts the cubane, resulting in shorter Fe–Fe distances within each cubane-half of FeMoco, compared to the $[MoFe_3S_4]^{3+}$ cluster (or even a $[Fe_4S_4]^{2+}$ cluster, e.g., from Ref. [37]).

Note that while the trispyrazolylborate (Tp) ligand on molybdenum in $[(Tp)MoFe_3S_4Cl_3]^{1-}$ (see Fig. 3) appears to be rather different than the molybdenum coordination

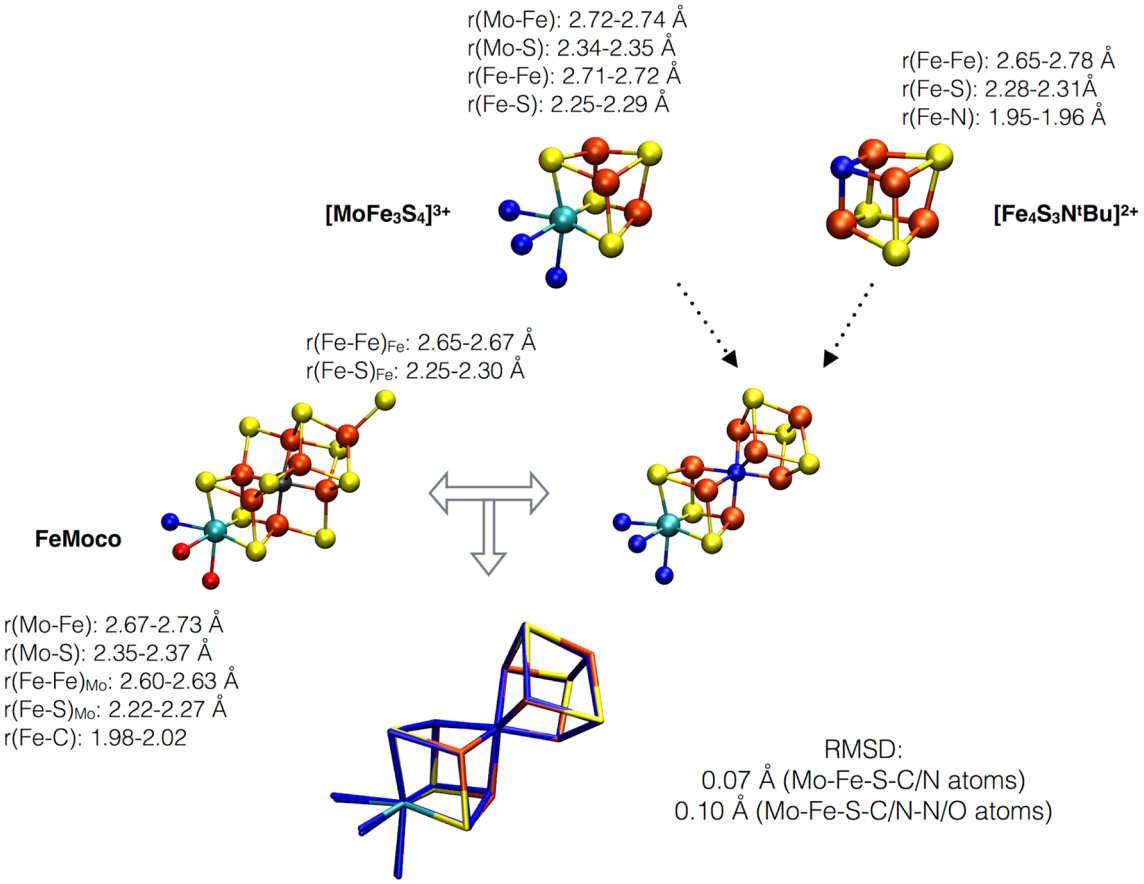

Fig. 4 Structural comparison of a $[MoFe_3S_4]^{3+}$ cubane (([(Tp)$MoFe_3S_4Cl_3]^{1-}$ from Ref. [36]), a $[Fe_4S_3N^tBu]^{2+}$ cubane (from Ref. [43]) and FeMoco. FeMoco can be imagined as a fusion of the two model cubanes (plus 3 sulfide bridges). A superposition of the Mo–Fe–S–C/N skeleton of the 2 fused cubanes and FeMoco gives a RMSD of 0.07 Å (Mo–Fe–S–C/N atoms) or 0.10 Å (including O/N atoms bonded to molybdenum as well, from either Tp or homocitrate/His)

environment in FeMoco (histidine and homocitrate ligation), both types of ligands result in a similarly distorted octahedral molybdenum coordination (RMSD of 0.16 Å for Mo–O–N atoms). $[MoFe_3S_4]$ cubanes with even more protein-like ligands have also been synthesized, including polycarboxylate ligands such as citrate and methyliminodiacetate [38, 39].

Synthetically coupling a $MoFe_3S_4$ cubane with a Fe_4S_3 fragment has so far not succeeded although various monosulfido and edge-bridged Mo–Fe–S double cubanes have come close to a FeMoco-like structure (the $[(Tp)_2Mo_2Fe_6S_9(SH)_2]_2$ cluster in Fig. 3 mimics almost perfectly the P-cluster topology [40]). Heteroatoms have also been incorporated in Fe–S based clusters (see recent review by Lee et al. [41]). Tatsumi et al. [42] were able to incorporate an oxygen atom in an $[Fe_8S_6O]$ cluster, which is reasonably close to mimicking the heteroatomic FeMoco environment, and Lee et al. [43, 44] succeeded in creating iron–sulfur–imido complexes, $[Fe_4S_{4-n}N_n]$. An $[Fe_4S_3N^tBu]$ complex (see Figs. 3, 4) is an analog of an $[Fe_4S_4]^{2+}$ cluster with a corner nitrogen instead of sulfur that was found to be a very good structural model for the Fe cubane-half of FeMoco (RMSD of 0.05 Å for Fe–S–N/C) with the corner nitrogen taking the role of the interstitial atom which results in a similar distortion of the cubane as the FeMoco carbide.

Incorporating a μ_6-carbide in a synthetic cluster remains a challenge. Nevertheless, it is clear that the Mo–Fe–S cubane structures synthesized, appear to be reasonable structural models for the molybdenum half of the FeMoco (sulfide instead of carbide at the cubane corner), while the well-known synthetic Fe–S cubane structures ($[Fe_4S_4]$ or $[Fe_4S_{4-n}X_n]$ structures) are quite reasonable models for the other half. Figure 4 shows a superposition of a $[MoFe_3S_4]^{3+}$ cubane by Holm et al. and the $[Fe_4S_3N^tBu]$ cubane by Lee et al. with FeMoco. This results in a low root-mean-square deviation (RMSD) of 0.07 Å for the Mo–Fe–S–C/N skeleton demonstrating the strong structural similarity of synthetic model cubanes with the biological cofactor.

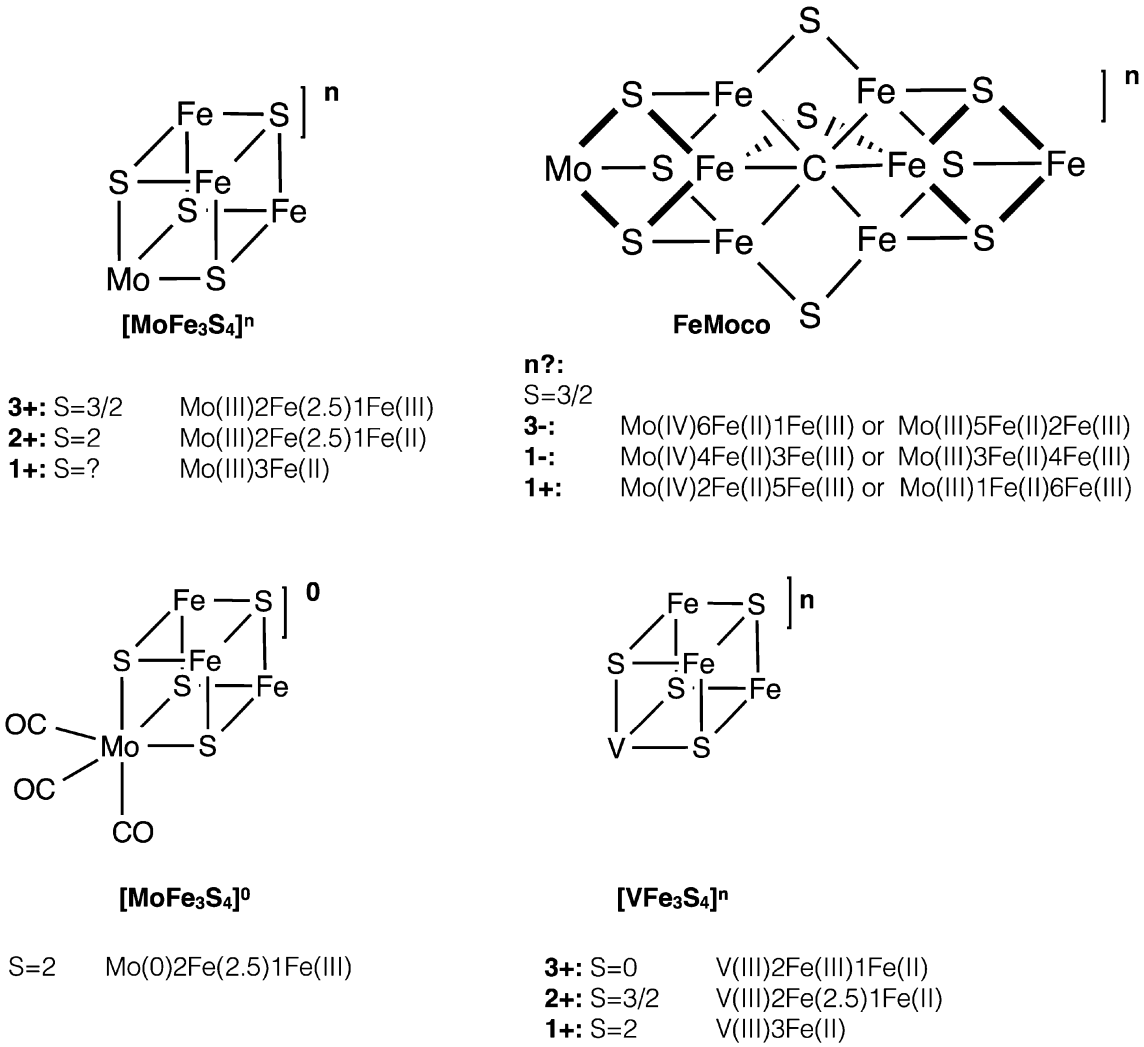

Fig. 5 Oxidation states and spin states of various synthetic $[MoFe_3S_4]$ and $[VFe_3S_4]$ cubanes, as well as the proposed oxidation state assignments of the resting state of FeMoco. It should be noted that for FeMoco, only the formal (and not the physical) oxidation states are shown. The actual physical oxidation state distribution is most likely more complicated due to electron delocalization [as seen in the Fe(2.5) pairs of the cubanes for example]

An obvious next question then is whether the synthetic cubanes have similarities at the electronic structure level as well.

Electronic structure and oxidation states

The resting state of the FeMoco cluster has long been known to have a spin state of $S = 3/2$ [45, 46]. The charge and metal oxidation states have not been confidently assigned, but there are generally three oxidation state assignments discussed in the literature: (1) 6Fe(II)1Fe(III) Mo(IV) [47]; (2) 4Fe(II)3Fe(III)Mo(IV) [18]; and (3) 2Fe(II)5Fe(III)Mo(IV) [48]. All 3 assignments are consistent with an $S = 3/2$ spin state and assume a closed-shell, diamagnetic, $S = 0$ Mo(IV) ion (see Fig. 5). A recent reassignment of the Mo oxidation state [49] is discussed in "Comparing the molybdenum oxidation state in MoFe protein vs Mo–Fe–S clusters". When written in terms of total charge on the cluster (an unambiguous way of presenting different charge models), with sulfur and carbon taken in their usual closed-shell forms, S^{2-} and C^{4-} (for electron-counting purposes only), the charges are $[MoFe_7S_9C]^{3-}$, $[MoFe_7S_9C]^{1-}$ and $[MoFe_7S_9C]^{1+}$, respectively. In view of biological iron–sulfur compounds being predominantly Fe(II) or Fe(III), it seems likely that the same applies to FeMoco.

The Mo(IV) assignment in FeMoco has been present in the nitrogenase literature since the 1980s. The assignment dates back to early Mo K-edge XAS studies by Hodgson

et al. and ^{95}Mo ENDOR studies by Hoffman et al., but the assignments were made prior to the first crystal structure of FeMoco was published. Mo–S derived bond lengths from the Mo EXAFS region suggested an oxidation state of either Mo(III) or Mo(IV) [5, 50]. Due to the significant core hole lifetime broadening at high energies, absorption edge positions did not give a clear indication of the Mo oxidation state. Later ^{95}Mo ENDOR experiments [51–53] indicated a small Mo hyperfine coupling in the protein and the data were interpreted as the molybdenum most plausibly being a closed-shell Mo(IV), rather than a $S = 3/2$ Mo(III) or $S = 1/2$ Mo(V). The authors acknowledged that the spin coupling schemes utilized were greatly simplified and that this assignment was tentative [52]. In 1988, a Mo L-edge XAS study [54] assigned the Mo atom in FeMoco as Mo(IV), when taking the ENDOR data into account, although a comparison of Mo–Fe–S based double cubanes and isolated FeMoco showed a strong similarity of the L_3 edges. However, a quantitative analysis of Mo L-edge data was prohibitive, due to both the proximity of the sulfur K-edge and the inadequacy of the available theoretical tools at that time. It seems that the initial Mo(IV) assignment of FeMoco influenced several studies on the electronic structure of FeMoco, both using experimental magnetic Mössbauer [18] and theoretical methods [48, 55–58].

The electronic structure of FeMoco is revisited in "Comparing the molybdenum oxidation state in MoFe protein vs Mo–Fe–S clusters".

Mo–Fe–S compounds with $[MoFe_3S_4]^n$ cores have been prepared with oxidation states of $n = 5+$, $4+$, $3+$, $2+$ and $1+$, either as single or double cubane compounds (see Fig. 5). The $[MoFe_3S_4]^{3+}$ oxidation level is the most easily accessible oxidation state and such cubanes are always found to have a total spin of $S = 3/2$ [59], while $[MoFe_3S_4]^{2+}$ cubanes (accessible by chemical reduction or a separate synthetic pathway) are $S = 2$ [60, 61]. Mössbauer spectroscopy has primarily been used to assign oxidation states in these cubanes, where the Mo oxidation state is assigned based on the individual Fe assignments, or sometimes only the average Fe oxidation state assignment using an empirical equation relating Fe oxidation state, isomer shift, and the total charge [6]. $[MoFe_3S_4]^{3+}$ has usually been assigned to have formal oxidation states of Mo(III) $Fe(III)_2Fe(II)$ (the physical oxidation states are discussed further later in this review). The change in isomer shift on going from $[MoFe_3S_4]^{3+}$ to $[MoFe_3S_4]^{2+}$ has further been interpreted as the redox event being primarily Fe based, hence giving $Mo(III)Fe(III)Fe(II)_2$. Cubane cores with the $[MoFe_3S_4]^{1+}$ oxidation state have also been prepared, although only as part of double cubanes [62]. The spin state of the $[MoFe_3S_4]^{1+}$ core has not been determined, but the change in average Mössbauer isomer shift again suggests a primarily Fe-based reduction and that the molybdenum remains in the Mo(III) oxidation state, suggesting Mo(III) $Fe(II)_3$. $[MoFe_3S_4]^{4+}$ and $[MoFe_3S_4]^{5+}$ cubanes have also been synthesized, but only with dithiocarbamate ligands [63]. Due to the potential ligand non-innocence, it is not clear whether their electronic structure is analogous to the more reduced cubanes [6].

Finally, we should mention that $[MoFe_3S_4]^0$ cores have also been prepared [64–66]. We mention them separately, as these compounds are not directly related to the more oxidized cores; they have only been prepared with CO ligation on the molybdenum and formally contain a Mo(0). The structures are very different from the $[MoFe_3S_4]^{3+/2+}$ cubanes, as the $[MoFe_3S_4]^0$ core has undergone trigonal elongation due to very weak bonding between the $[Mo(CO)_3]^0$ unit and the $[Fe_3S_4]^0$ unit (Mo–Fe distances in $[MoFe_3S_4]^0$ increase to ~3.2 Å compared to 2.7 Å in $[MoFe_3S_4]^{3+}$ cubanes). Fe oxidation states of the $[Fe_3S_4]^0$ unit have been assigned as 2 Fe(III) and 1 Fe(II) and the electronic structure can be described as mixed-valence delocalized Fe(2.5)–Fe(2.5) pair antiferromagnetically coupled to a Fe(III) ion.

It is worth noting that analogous heterometal cubanes with vanadium and tungsten have also been synthesized [6]. The $[VFe_3S_4]^{2+}$ core is isoelectronic to $[MoFe_3S_4]^{3+}$, has the same spin $S = 3/2$ ground state and is approximately isostructural, but has been found to have a more reduced Fe-part [67], suggesting an oxidation state assignment of $V(III)Fe(II)_2Fe(III)$. Other $[VFe_3S_4]^n$ cubanes have also been synthesized and characterized [68] and found to have Fe-based reductions with the vanadium atom assigned as V(III) (d^2 configuration). These compounds are potentially relevant structural models for the iron–vanadium cofactor (FeVco) that has been suggested to be analogous to FeMoco [69], albeit this still awaits crystallographic verification.

Besides standard Mössbauer spectroscopy as a means to gain insight into the Fe electronic structure of these cubanes, various magnetic spectroscopies have been employed. EPR spectroscopy and magnetic susceptibility measurements were used to determine a ground spin state of $S = 3/2$ in the $[MoFe_3S_4]^{3+}$ cubanes [59]. Both $[MoFe_3S_4]^{3+}$ and MoFe protein were in fact found to give rise to very similar EPR spectra [60]. A study by Mascharak et al. [60] in 1983 employed many different spectroscopies on $[MoFe_3S_4]^{3+}$ single and double cubane compounds and properties were compared to MoFe protein. The Mössbauer spectra of a $[MoFe_3S_4]^{3+}$ cubane with catecholate ligands gave rise to a mean Fe oxidation state of $Fe^{2.67+}$ which corresponds to a formal assignment of $Mo(III)Fe(III)_2Fe(II)$. Two different Fe species could be successfully fit to the spectrum, with an intensity ratio of 2:1. Later Mössbauer studies of other $[MoFe_3S_4]^{3+}$ compounds have generally resulted in a fit of two different Fe species, with the more

intense species sometimes (not always resolved) having a slightly larger isomer shift, thus suggesting Fe assignments of a mixed-valence delocalized Fe(2.5)–Fe(2.5) pair (as are commonly observed in iron–sulfur cubane clusters) and a Fe(III) ion. Computed Mössbauer parameters of another $[MoFe_3S_4]^{3+}$ core support this description [49]. When a magnetic field was applied to the catecholate-ligated $[MoFe_3S_4]^{3+}$ compound in the Mascharak et al. study [60], two magnetic subsites were revealed, again with an intensity ratio of 2:1. Analyzing the splittings as a function of field strength was indicative of antiparallel spin coupling of the Fe ions in the cubane with the more intense subsite having a negative hyperfine field, hence being the majority spin. The majority spin species can nowadays plausibly be interpreted as a mixed-valence delocalized Fe(2.5)–Fe(2.5) pair, with the minority spin being a single Fe(III) ion. We note that while the authors of the magnetic Mössbauer studies also considered a Mo(IV)1Fe(III)2Fe(II) interpretation as a possibility, this seems unlikely in view of the cases where well-resolved Mössbauer spectra of $[MoFe_3S_4]^{3+}$ cubanes show the more intense Fe species with a higher isomer shift. Further, such an assignment is also inconsistent with theoretical calculations [70, 71], as noted below.

Mascharak et al. highlighted in their study the similarities in electronic structure, as determined by the magnetic spectroscopies, of synthetic cubanes vs. MoFe protein, ranging from a similar electron delocalization, antiparallel spin coupling, hyperfine couplings and similar EPR spectra.

Cook and Karplus [70, 71] were the first to attempt a detailed electronic structure analysis of a $[MoFe_3S_4]^{3+}$ cubane by theoretical calculations. Broken-symmetry MS-$X\alpha$ calculations were performed which resulted in an electronic structure picture consisting of antiferromagnetically coupled Fe atoms, mixed-valence delocalization and a molybdenum(III) assignment with an unusual ($\uparrow\uparrow\downarrow$) configuration and low spin population.

As the discussion above highlights, the comparison of FeMoco and Mo–Fe–S cubanes goes beyond mere molecular structure similarity. Mixed-valence delocalization, as well as antiferromagnetic spin coupling of Fe, is apparent in the electronic structure for both FeMoco and the Mo–Fe–S cubanes. Further, the EPR spectra and Mössbauer properties are similar. Yet, the oxidation state of molybdenum is almost exclusively assigned as Mo(III) in the Mo–Fe–S cubane literature, regardless of cubane oxidation state (indicating redox processes taking place at Fe), while the molybdenum in FeMoco has (until very recently) always been assigned as a closed-shell $S = 0$ Mo(IV) in the nitrogenase literature. This apparent discrepancy prompted us to probe directly the molybdenum oxidation state in both MoFe protein and Mo–Fe–S clusters, using a combined Mo XAS spectroscopy and theoretical approach.

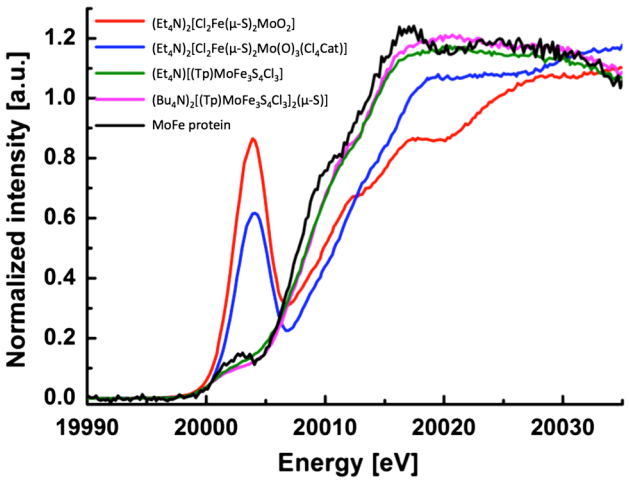

Fig. 6 The pre-edge and main absorption Mo XAS edges of synthetic Mo–Fe–S compounds and MoFe protein. Dimer compounds (*red* and *blue lines*) are Mo(V) compounds, $[(Tp)MoFe_3S_4Cl_3]^{1-}$ (*green*) and $[(Tp)MoFe_3S_4Cl_3]_2(\mu\text{-}S)]$ (*pink*) have been assigned as Mo(III). Adapted from Ref. [49] with permission of The Royal Society of Chemistry

Comparing the molybdenum oxidation state in MoFe protein vs Mo–Fe–S clusters

In a recent article by some of us [49], we revisited the molybdenum oxidation state assignment in FeMoco by a combined experimental and theoretical approach. By performing high-energy resolution fluorescence detected (HERFD) Mo X-ray absorption spectroscopy on MoFe protein and selected model compounds, we obtained higher resolution Mo XAS spectra than had been possible before. Two of the model compounds measured were Mo–Fe–S cubane compounds, originally described by Holm et al. One was a $[MoFe_3S_4]^{3+}$ cubane with a trispyrazolylborate (Tp) ligand on the molybdenum and the other a $([MoFe_3S_4]^{3+})_2$ double cubane with Tp on each molybdenum.

Since the molybdenum coordination environment in MoFe protein and the two cubane complexes is very similar, the absorption edge position should be a good indicator of a difference in oxidation state [72]. As seen in Fig. 6, both the pre-edge and the main absorption edge are very similar in MoFe protein and the 2 cubane complexes, with MoFe protein having a rising edge if anything, to slightly lower energy than either cubane model. This is in contrast to the absorption edges of the Mo(V) compounds, which have absorption edges at much higher energies. We note that an appropriate Mo(IV) reference model complex was not available for the initial study. However, we note that the Mo(IV) possibility for FeMoco can be ruled out due to the fact that the rising edge of MoFe protein appears to slightly lower energy than the Mo(III) cubane references. A Mo(IV) complex should have a rising edge between

that of the Mo(III) and Mo(V) model complexes. Hence based on these data, a Mo(III) assignment was found to be most appropriate for FeMoco. Further, we note that in the original study, careful radiation damage studies were carried out, and the published data correspond to undamaged MoFe protein.

Due to the similarities in the Mo HERFD XAS data for the $[MoFe_3S_4]^{3+}$ cubanes and FeMoco, a Mo(III) assignment for FeMoco appears most appropriate based only on empirical considerations. However, we note that, in the initial study, we went beyond the simple fingerprint approach and computed the Mo XAS pre-edges using time-dependent density functional theory (TDDFT) from broken-symmetry SCF solutions of model compounds and a 225-atom FeMoco model. Computed pre-edges of model compounds and our cofactor model were found to be in excellent agreement with the experimental pre-edges and a rigorous orbital analysis of broken-symmetry SCF solutions of cubane model compounds and FeMoco revealed a d^3 configuration at the molybdenum, consistent with Mo(III) for both cubanes and FeMoco. Curiously, we found the molybdenum configuration to have an unusual low spin configuration ($\uparrow\uparrow\downarrow$) (apparently analogous to the one found by Cook and Karplus earlier for a similar model system [71]), that we have referred to as a non-Hund configuration. This configuration, combined with covalency effects, appears to be the reason for a small spin population at molybdenum (ranging from -0.1 to -0.6, depending on the DFT method) compared to an idealized value of 3.0 for an ionic Mo(III). This unusual feature may have been missed in previous DFT studies of FeMoco and appears to have not been explored further for Mo–Fe–S systems since the study by Cook and Karplus.

Due to limitations of a single-reference quantum chemistry approach (whether DFT or MS-$X\alpha$), it is unfortunately not possible to tell whether the non-Hund configuration in FeMoco or Mo–Fe–S cubanes represents a genuine excited spin state of the molybdenum or whether the configuration arises due to spin-canting effects in the cubane system. A multiconfigurational ab initio approach may help to shed some light on the matter. Such approaches have recently been applied to the exchange-coupled manganese-based oxygen-evolving complex [73] as well as Fe_4S_4 cubanes [74]. It is clear that a magnetic spectroscopic approach will be needed for direct experimental evidence of the spin structure at the molybdenum. What the DFT calculations reveal, however, is that the unusual molybdenum configuration can only be stabilized due to spin coupling with the iron atoms, and a localized orbital analysis suggests that the molybdenum electrons reside in partially bonding orbitals with Fe, indicative of a double-exchange effect between Mo and Fe. A spin-coupled Mo(III) is probably the best description of molybdenum in FeMoco for now, while the details of the Mo–Fe interaction are not understood.

The Mo HERFD XAS study was unfortunately not able to establish the total charge on the FeMoco cluster; however, it was established that for all 3 charges considered for FeMoco, the unusual Mo(III) configuration remained. For the $[MoFe_7S_9C]^{1-}$ model, the electronic structure in the Mo-cubane fragment was found to be analogous to the electronic structure of the $[MoFe_3S_4]^{3+}$ cubane, in either the $[(Tp)MoFe_3S_4Cl_3]^{1-}$ cluster or the double cubane $[(Tp)MoFe_3S_4Cl_3]_2(\mu\text{-}S)]$. This is illustrated in Fig. 7, which shows a preliminary generalized electronic structure diagram for a Mo–Fe–S cubane, with either a sulfide or carbide corner atom: i.e., $[MoFe_3S_3C]^{1+}$ or $[MoFe_3S_4]^{3+}$. The two cubanes share the following features: the unusual non-Hund configuration at molybdenum, a mixed-valence Fe(2.5)–Fe(2.5) pair and an antiferromagnetically coupled Fe(III). Computed Mössbauer parameters of $[(Tp)MoFe_3S_4Cl_3]^{1-}$ are in good agreement with experimental values and thus support the basic features of this diagram [49].

Finally, a recent Mo L-edge study by us reexamined previous Mo L-edge data [54] on isolated FeMoco and double cubane compounds and presented new data on MoFe protein [75]. This study provides further support for the Mo(III) assignment in FeMoco; the Mo(III) assignment holds for both the NMF-isolated cofactor and the protein-bound cofactor.

Reactivity of structural model compounds: relation to biological reactivity

The Mo–Fe–S cubane compounds were synthesized to serve both as biomimetic structural models of FeMoco and as part of exploratory synthetic chemistry. It became clear, however, that a subset of these models also exhibited interesting reactivity, possibly relevant to the reactivity of FeMoco.

Nitrogenase is known to act as a proton-reducing catalyst when no N_2 substrate is available and this seems to be nature's way of terminating the electron-transfer pathway when no substrate is present. What is also known, but not understood, is the obligatory H_2 formation accompanying NH_3 formation. Dean, Hoffman, Seefeldt et al. [76, 77] have recently proposed reductive elimination of hydrides occurring at the FeMoco as an explanation of this phenomenon.

Already in 1980 [78], it was found that some reduced Mo–Fe–S cubanes were capable of H_2 evolution when protonated, and in 1983, a very detailed kinetic analysis was performed [79]. The double cubane cluster $[Mo_2Fe_6S_8(SPh)_9]^{5-}$ was found to evolve dihydrogen slowly from protonation agents like PhSH and Et_3NH^+ with a yield of 100 % (based on electron count). This

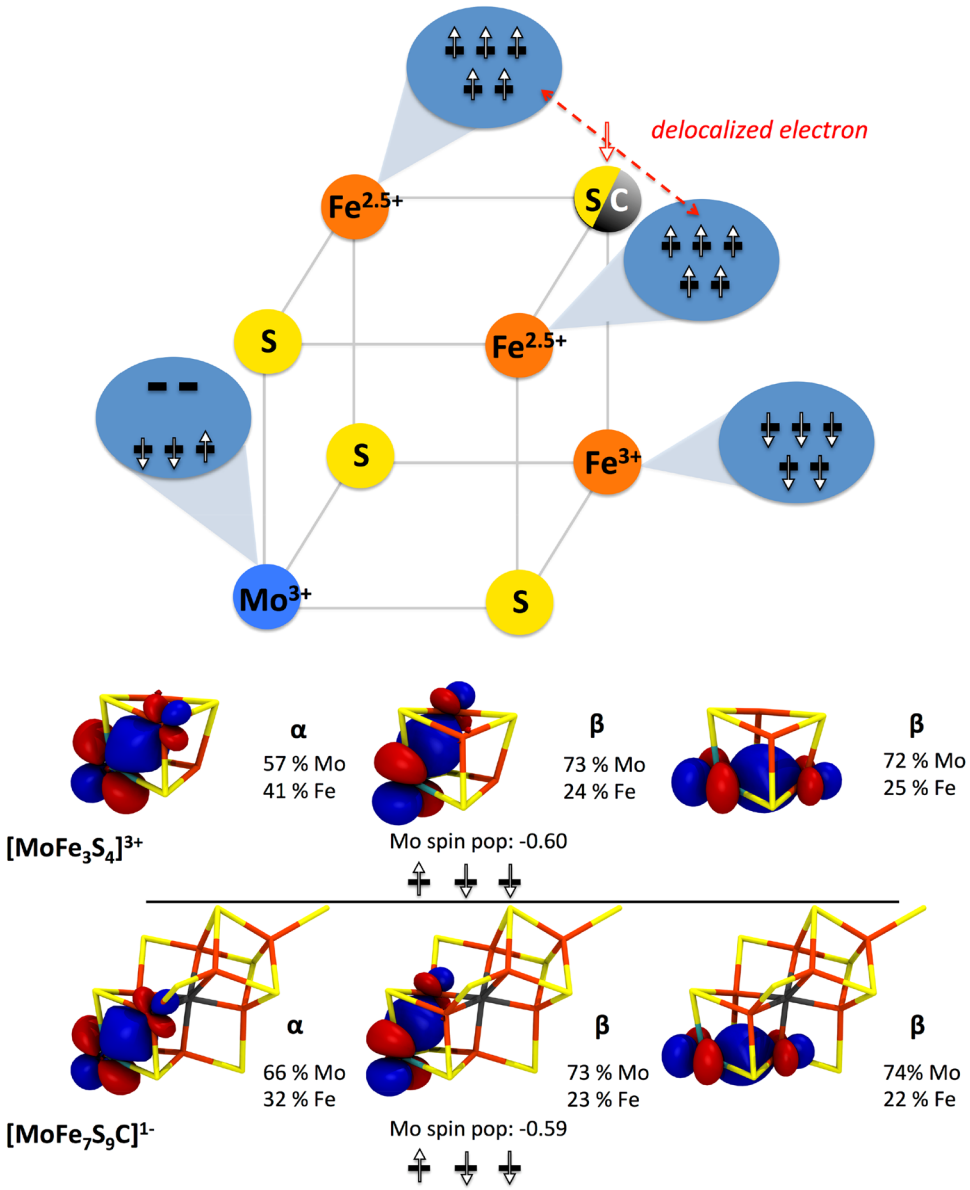

Fig. 7 *Upper* Generalized electronic structure diagram for $[MoFe_3S_3C]^{1+}$ and $[MoFe_3S_4]^{3+}$ cubanes. *Lower* Localized occupied t_{2g} orbitals of molybdenum in $[MoFe_3S_4]^{3+}$ cubane and FeMoco model $[MoFe_7S_9C]^{1-}$. Reproduced from Ref. [49] with permission of The Royal Society of Chemistry

reactivity was connected to the property of the double cubane being able to undergo 2 low-potential 1-electron reductions [potentials given vs. saturated calomel electrode (SCE)]:

$$[Mo_2Fe_6S_8(SR)_9]^{3-} \Leftrightarrow [Mo_2Fe_6S_8(SR)_9]^{4-} \Leftrightarrow [Mo_2Fe_6S_8(SR)_9]^{5-}$$

$$-1.02\ V \qquad -1.23\ V \qquad (vs.\ SCE)$$

$[Mo_2Fe_6S_8(SR)_9]^n$ is thus a rare example of a single molecule that can act as a carrier of 2 electrons to be delivered to a substrate (here proton). H_2 evolution from a $[Fe_4S_4]$ cubane compound, $[Fe_4S_4(SPh)_4]^{3-}$, was also found, albeit with much lower yields (11–31 %). This was attributed to the reaction of 2 cubanes per H_2 formed, as $[Fe_4S_4(SPh)_4]^{3-}$ is only a 1-electron carrier [80].

A detailed kinetic study [79] of $[Mo_2Fe_6S_8(SPh)_9]^n$ gave experimental rate laws and proposed a preliminary mechanism involving a likely hydride intermediate prior to H_2 evolution. The double cubane, $[Mo_2Fe_6S_8(SPh)_9]^{5-}$, can be thought of as 2 $[MoFe_3S_4]^{2+}$ cubanes and thus each is a 1-electron carrier (w.r.t. $[MoFe_3S_4]^{3+}$). It was suggested that it is the 2-electron carrier feature of these

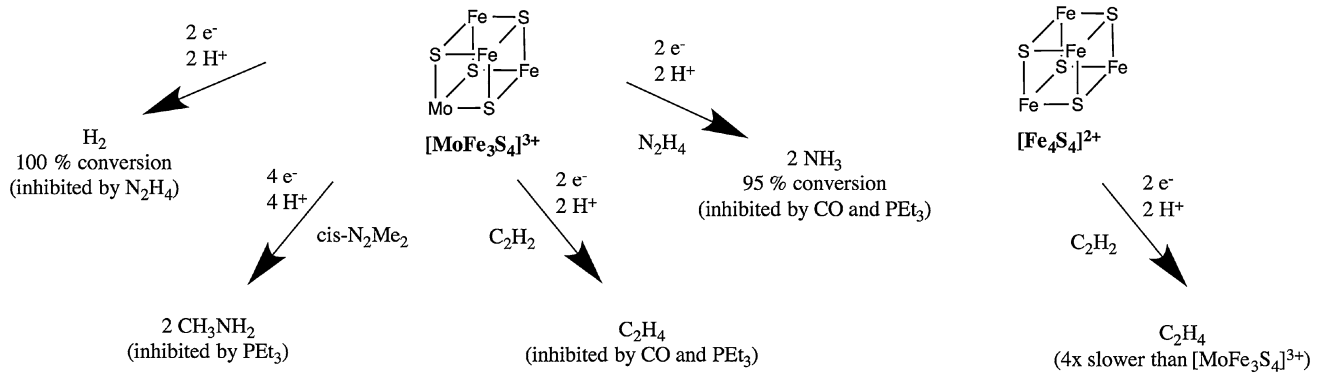

Fig. 8 The catalytic activity of $[MoFe_3S_4]^{3+}$ cores compared to $[Fe_4S_4]^{2+}$ cores for nitrogenase substrates

double cubanes that is the central property here, as the 1-electron reduction potential of $[Mo_2Fe_6S_8(SPh)_9]^{3-}$ and $[Fe_4S_4(SPh)_4]^{3-}$ is rather similar (−1.02 vs. −1.04 V in DMF, vs. SCE).

Since FeMoco can also be described as a double cubane (although an unusual carbon-ligated one, $[MoFe_3S_3]$-C-$[Fe_4S_3]$), it seems plausible that this is an important property of the cofactor, allowing it to perform multi-electron chemistry (for example H_2 evolution, and N_2 reduction).

The H_2 evolution chemistry of synthetic Mo–Fe–S cubanes has not been explored much more since then, although we note in this context the isolated FeMo cofactor studies by Pickett et al. [80–82]. These studies demonstrated the H_2 evolution capabilities of the NMF-isolated cofactor (85 % conversion of electrons) and proposed hydride intermediates. Also noteworthy is recent work of Kanatzidis et al. [83] where $[Mo_2Fe_6S_8X_9]$ double cubanes were incorporated into a chalcogenide framework. Utilizing a $[Ru(bpy)_3]^{2+}$ photosensitizer, the chalcogel was capable of photocatalytic H_2 production.

Mo–Fe–S cubanes have also been found to be capable of other small molecule reactivity, some of which are nitrogenase-related substrates (Fig. 8). In studies by Coucouvanis et al. [84, 85] $[MoFe_3S_4]^{3+}$ cubanes (as well as $[VFe_3S_4]^{2+}$ [86]) were found to be active catalysts for the reduction of hydrazine to ammonia [87, 88], acetylene to ethylene [89] and *cis*-dimethyldiazene to methylamine [90]. These studies were conducted using cobaltocene and 2,6-lutidinium chloride as external sources of electrons and protons.

The catalytic $2e^-$ reduction of hydrazine, N_2H_4, to ammonia was accomplished by different $[MoFe_3S_4]^{3+}$ cubanes in very detailed studies where $[Fe_4S_4Cl_4]^{2-}$ clusters were found to be inactive. Through explorations of various ligands to the molybdenum atom, the most effective catalysts were found to be compounds with polycarboxylate ligands (such as citrate) on molybdenum. It was hypothesized that this ligand preference could derive from citrate protonation opening a free coordination site for hydrazine and the polycarboxylate acting as a proton shuttle. This observation is of potential relevance to the enzymatic system as molybdenum-bound homocitrate in FeMoco has been found to be crucial for dinitrogen reduction. Studies where homocitrate was replaced with other polycarboxylate ligands dramatically reduced FeMoco activity [91, 92].

In the $[MoFe_3S_4]^{3+}$ cubane studies, strong binding ligands at molybdenum, like PEt_3 were found to inhibit the reaction, presumably by blocking all six coordination sites, strongly suggesting molybdenum as the site of binding for hydrazine. Phenylhydrazine ligated to the molybdenum of a $[MoFe_3S_4]^{3+}$ was also found by X-ray crystallography [88].

CO was found to inhibit hydrazine reduction, although CO has only been found to bind to the 1-electron reduced cubane $[MoFe_3S_4]^{2+}$, with the site of binding tentatively assigned to molybdenum [15]. In this context, we note that very recently a crystal structure of CO-inhibited MoFe protein was published. The structure shows CO replacing a sulfur-bridge in FeMoco, bound to 2 Fe atoms, i.e., a rather different type of inhibition than proposed for synthetic Mo–Fe–S cubanes.

A later study by Coucouvanis et al. [90] demonstrated the catalytic $4e^-$ reduction of *cis*-dimethyldiazene by $[MoFe_3S_4]^{3+}$ to methylamine, the first example of reducing a N=N bond. Again strong evidence was presented for the binding and activation of the substrate at molybdenum by phosphine inhibition studies. $[Fe_4S_4Cl_4]^{2-}$ showed essentially no reactivity. The sole product, methylamine, bound at the molybdenum, was found by X-ray crystallography. A difference between the synthetic system and the enzyme was also revealed as the enzyme reduces *cis*-dimethyldiazene to a mixture of products: ammonia, methane and methylamine.

It should be made clear that $[MoFe_3S_4]$ (or $[VFe_3S_4]$) cores have not been found capable of $6e^-/8e^-$ N_2 reduction, which obviously is a much more difficult reaction.

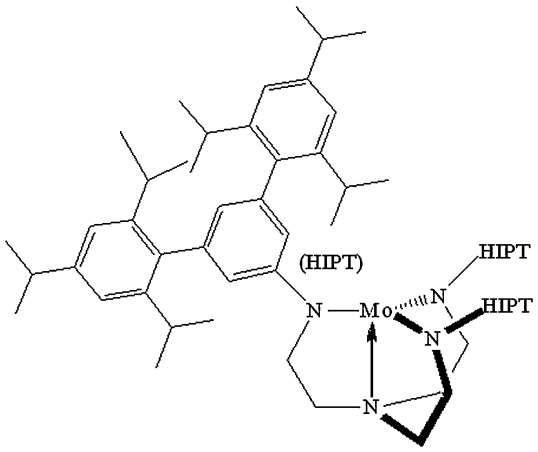

Fig. 9 The Mo(III) core of [$HIPTN_3N$]Mo complexes

Coucouvanis has suggested that the catalytic activity of [$MoFe_3S_4$] cores could be an indicator of the direct involvement of the molybdenum atom in the mechanism at the hydrazine level, by substrate migration [93]. It is possible that activation of N_2 by these types of clusters in fact requires a large cluster such as FeMoco (i.e., a double cubane fused by an interstitial carbide) not present in any of the synthetic single or double cubanes discussed here.

Functional models for N_2 reduction have a longer history than the structural Mo–Fe–S systems. The first nitrogen complex reported by Allen and Senoff in 1965, $[Ru(NH_3)_5(N_2)]^+$, was prepared by treating $RuCl_3(H_2O)_3$ with excess hydrazine; hydrazine was the reducing agent and (presumably) the source of ammonia and nitrogen through disproportionation [94]. This discovery initiated a search not only for more nitrogen complexes, but in particular nitrogen complexes that would generate ammonia under some set of conditions, preferably catalytically. Among the groups active in the search included groups based in England, Japan, the United States, and the Soviet Union [95–101]. The first dinitrogen complexes of molybdenum (Mo(0)) were prepared by Hidai and his group in 1969. The first (stoichiometric) generation of ammonia from Mo(0) and W(0) complexes through addition of acid was published by Chatt and Richards in 1975. The first catalytic reduction of dinitrogen published by Shilov and his group employed a source of molybdenum and a strong reducing agent in methanol; however, the primary reduction product in this system is hydrazine, which is then disproportionated to nitrogen and ammonia. Typically a 10:1 mixture of hydrazine and ammonia is reportedly formed.

A breakthrough molybdenum-based catalyst for N_2 reduction was published by Schrock et al. in 2003 [102–104]. The relevant Mo complexes contain the $[HIPTN_3N]^{3-}$ ligand, where HIPT = 3,5-(2,4,6-i-$Pr_3C_6H_2)_2C_6H_3$ (HexaIsoPropylTerphenyl; Fig. 9), a ligand that was designed to prevent formation of relatively stable and unreactive bimetallic (Mo–N=N–Mo) complexes, maximize steric protection of a metal coordination site in a monometallic species, and provide increased solubility in nonpolar solvents. Eight of the proposed intermediates in a hypothetical "Chatt-like" reduction of dinitrogen were prepared and characterized. These include paramagnetic **Mo**(N_2), diamagnetic [**Mo**$(N_2)]^-$, diamagnetic **Mo**–N=N–H, diamagnetic [**Mo**=N–NH_2]BAr'_4 (Ar′ = 3,5-$(CF_3)_2C_6H_3$), diamagnetic **Mo**≡N, diamagnetic [**Mo**=NH]BAr'_4, paramagnetic [**Mo**(NH_3)]BAr'_4, and paramagnetic [**Mo**(NH_3)] (where **Mo** is [$HIPTN_3N$]Mo). In the catalytic reaction, which involves $Cr(\eta^5\text{-}C_5Me_5)_2$ as the reducing agent and lutidinium BAr'_4 as the proton source (in heptane), approximately 7.5 equivalents of ammonia are formed per Mo. The only other product is hydrogen, with the ratio of ammonia to hydrogen being ~2:1, as found in FeMoco. The system has a well-characterized [105–107] redox cycle, starting with a Mo(III) state in **Mo**(N_2), with protons and electrons being added alternately, except possibly the first of each in a proton-couple electron transfer to give **Mo**–N=N–H from **Mo**(N_2) [108]. In this mechanism, the distal nitrogen is hydrogenated first, releasing the first NH_3 molecule to give **Mo**≡N, while the second equivalent of ammonia is formed from [**Mo**(NH_3)] through displacement by nitrogen in a six-coordinate [**Mo**(NH_3)] (N_2) intermediate. Molybdenum is found in oxidation states between Mo(III) to Mo(VI). The proposed catalytic reduction mechanism has been fully confirmed through computational mechanistic studies that involve the full ligand [109].

A second Mo(0)-based bimetallic catalyst was found by Nishibayashi and coworkers to reduce dinitrogen to ammonia with $Co(\eta^5\text{-}C_5H_5)_2$ as the reducing agent and lutidinium triflate as the proton source to give a maximum of ~12 equivalents of ammonia per Mo [110]. No catalytically viable intermediates have been isolated and the detailed mechanism of the reduction remains obscure. It seems unlikely that Mo(0) is the lowest oxidation state, since $Co(\eta^5\text{-}C_5H_5)_2$ is not a strong enough reducing agent to form Mo(0).

Fe-based catalysts for N_2 reduction were recently reported by Peters et al. [111, 112]. The compounds are phosphine-supported trigonal geometries with axial coordination to iron by boron, silicon or carbon. The compounds bind N_2 in the other axial position trans to B, Si or C; the B- and C-containing systems catalyze reduction to NH_3. The conditions are relatively severe with the reducing agent being KC_8 and the proton source being $H(Et_2O)_2BAr'_4$ in THF at −78 °C. Approximately 7 equivalents of ammonia and ~15 equivalents of hydrogen are formed per Fe in the system in which the ligand contains boron *trans* to the nitrogen-binding site. It has been suggested that the atom *trans* to nitrogen in the TBP complex provides a "flexible" interaction with the metal *trans* to the N_2 binding site [113],

and therefore is crucial to catalytic activity. However, the ligand in which a carbon atom is *trans* to the nitrogen-binding site gives only ~5 equivalents of ammonia per Fe, i.e., less than the system that contains boron.

None of the functional Fe or Mo systems has any structural or mechanistic feature that could be said to be "biomimetic" beyond the obvious, i.e., the presence of Fe or Mo. The only distant possibility is the trigonal arrangement of sulfur atoms around both Fe and Mo in FeMoco. Molybdenum and iron-based homogenous systems for N_2 reduction were recently reviewed by Holland et al. [114].

Uncovering the role of the molybdenum

The molecular structure of resting state FeMoco can be considered complete and recent studies in our group are moving toward a clear assignment of the charge. Combining this information with the Mo(III) assignment and electronic structure calculations gives us a simplified, but useful picture of the metal oxidation states in the cofactor. Perhaps the most important result of recent studies is that the cofactor can now be connected with the rich structural information of other Mo–Fe–S clusters. Due to complexity of the cofactor, however, the structural information that we now possess, provides only the first step toward understanding how FeMoco operates.

Molybdenum is clearly an essential part of FeMoco as is known from enzymes formed in molybdenum-deficient environments. What is still not understood is the role of the molybdenum in the mechanism of nitrogen reduction. It is important to reiterate that there is still no direct evidence for the binding site of N_2. Current biochemical data favor one of the irons in the Mo cubane, Fe6 (X-ray structure labeling), as the binding site, mainly due to loss of activity upon increasing the bulkiness (mutating α-70 Val into Ile) of the residue directly above Fe6 [115, 116]. If molybdenum is not the binding site then the atom may play a role in tuning the redox potential of the cofactor as a whole (or even a specific iron atom). Alternatively the role of the Mo may be to modify the electronic structure of the cofactor to facilitate binding or protonation of substrate. As suggested by studies by Coucouvanis et al. on the catalytic activity of $[MoFe_3S_4]^{3+}$ cubanes for hydrazine and *cis*-dimethyldiazene reduction, the molybdenum might also play a direct role in later stages of nitrogen reduction.

The observation that molybdenum (or vanadium) appears to never change oxidation state upon reduction of Mo–Fe–S systems, as revealed by the electron-transfer chemistry of synthetic cubanes and also suggested for FeMoco, may even be an important property of the heterometal in the cluster. This would be in sharp contrast to the Schrock/Chatt cycles for nitrogen reduction, however, where molybdenum-based redox is crucial to catalytic activity.

The next challenges in FeMoco research will be to gain a better understanding of the electronic structure of FeMoco and particularly to understand its relation to reactivity. This will involve a characterization of the redox states of FeMoco (as FeMoco requires at least 3 reduction events prior to N_2 binding), where Fe-based hydrides have been proposed to be an important feature of the redox process [76, 77], as well as gathering direct experimental evidence of the N_2 binding site and the nature of binding and activation. Overcoming these challenges will signify a real step toward an understanding of biological dinitrogen reduction.

Acknowledgments RB, FN and SD acknowledge the Max Planck Society for Funding. SD acknowledges funding from the European Research Council under the European Union's Seventh Framework Programme (FP/2007–2013) ERC Grant Agreement No. 615414. RB acknowledges support from the Icelandic Research Fund, grant no. 141218051.

References

1. Burgess BK, Lowe DJ (1996) Chem Rev 96:2983–3012
2. Howard JB, Rees DC (1996) Chem Rev 96:2965–2982
3. Spatzal T, Aksoyoglu M, Zhang L, Andrade SLA, Schleicher E, Weber S, Rees DC, Einsle O (2011) Science 334:940
4. Lancaster KM, Roemelt M, Ettenhuber P, Hu Y, Ribbe MW, Neese F, Bergmann U, DeBeer S (2011) Science 334:974–977
5. Cramer SP, Hodgson KO, Gillum WO, Mortenson LE (1978) J Am Chem Soc 100:3398–3407
6. Lee SC, Holm RH (2004) Chem Rev 104:1135–1158
7. Malinak SM, Coucouvanis D (2001) Progress in inorganic chemistry. 49:599–662
8. Wolff TE, Berg JM, Warrick C, Hodgson KO, Holm RH, Frankel RB (1978) J Am Chem Soc 100:4630–4632
9. Wolff TE, Berg JM, Hodgson KO, Frankel RB, Holm RH (1979) J Am Chem Soc 101:4140–4150
10. Wolff TE, Berg JM, Power PP, Hodgson KO, Holm RH (1980) Inorg Chem 19:430–437
11. Wolff TE, Power PP, Frankel RB, Holm RH (1980) J Am Chem Soc 102:4694–4703
12. Christou G, Garner CD (1980) J Chem Soc Dalton Trans, pp 2354–2362
13. Armstrong WH, Holm RH (1981) J Am Chem Soc 103:6246–6248
14. Armstrong WH, Mascharak PK, Holm RH (1982) J Am Chem Soc 104:4373–4383
15. Mascharak PK, Armstrong WH, Mizobe Y, Holm RH (1983) J Am Chem Soc 105:475–483
16. Antonio MR, Teo BK, Orme-Johnson WH, Nelson MJ, Groh SE, Lindahl PA, Kauzlarich SM, Averill BA (1982) J Am Chem Soc 104:4703–4705
17. Kim J, Rees DC (1992) Science 257:1677–1682
18. Yoo SJ, Angove HC, Papaefthymiou V, Burgess BK, Münck E (2000) J Am Chem Soc 122:4926–4936
19. Andres H, Bominaar EL, Smith JM, Eckert NA, Holland PL, Münck E (2002) J Am Chem Soc 124:3012–3025
20. Smith JM, Lachicotte RJ, Pittard KA, Cundari TR, Lukat-Rodgers G, Rodgers KR, Holland PL (2001) J Am Chem Soc 123:9222–9223

21. Smith JM, Lachicotte RJ, Holland PL (2003) J Am Chem Soc 125:15752–15753
22. Vela J, Stoian S, Flaschenriem CJ, Münck E, Holland PL (2004) J Am Chem Soc 126:4522–4523
23. Holland PL (2005) Can J Chem 83:296–301
24. Yu Y, Smith JM, Flaschenriem CJ, Holland PL (2006) Inorg Chem 45:5742–5751
25. Deng H, Hoffmann R (1993) Angew Chem Int Ed 32:1062–1065
26. Stavrev KK, Zerner MC (1998) Int J Quantum Chem 70:1159–1168
27. Dance I (1996) JBIC 1:581–586
28. Siegbahn PEM, Westerberg J, Svensson M, Crabtree RH (1998) J Phys Chem B 102:1615–1623
29. Rod TH, Nørskov JK (2000) J Am Chem Soc 122:12751–12763
30. Lovell T, Li J, Case DA, Noodleman L (2002) J Am Chem Soc 124:4546–4547
31. Tyson MA, Coucouvanis D (1997) Inorg Chem 36:3808–3809
32. Han J, Beck K, Ockwig N, Coucouvanis D (1999) J Am Chem Soc 121:10448–10449
33. Coucouvanis D, Han J, Moon N (2002) J Am Chem Soc 124:216–224
34. Einsle O, Tezcan FA, Andrade SLA, Schmid B, Yoshida M, Howard JB, Rees DC (2002) Science 297:1696–1700
35. Einsle O (2014) J Biol Inorg Chem 19:737–745
36. Fomitchev DV, McLauchlan CC, Holm RH (2002) Inorg Chem 41:958–966
37. Lo W, Huang S, Zheng SL, Holm RH (2011) Inorg Chem 50:11082–11090
38. Coucouvanis D, Demadis KD, Kim CG, Dunham RW, Kampf JW (1993) J Am Chem Soc 115:3344–3345
39. Demadis KD, Coucouvanis D (1995) Inorg Chem 34:436–448
40. Zhang Y, Zuo JL, Zhou HC, Holm RH (2002) J Am Chem Soc 124:14292–14293
41. Lee SC, Lo W, Holm RH (2014) Chem Rev 114:3579–3600
42. Ohta S, Ohki Y, Hashimoto T, Cramer RE, Tatsumi K (2012) Inorg Chem 51:11217–11219
43. Chen XD, Duncan JS, Verma AK, Lee SC (2010) J Am Chem Soc 132:15884–15886
44. Chen XD, Zhang W, Duncan JS, Lee SC (2012) Inorg Chem 51:12891–12904
45. Munck E, Rhodes H, Ormejohnson WH, Davis LC, Brill WJ, Shah VK (1975) Biochim Biophys Acta 400:32–53
46. Zimmermann R, Ormejohnson WH, Munck E, Shah VK, Brill WJ, Henzl MT, Rawlings J (1978) Biochim Biophys Acta 537:185–207
47. Lee H, Hales BJ, Hoffman BM (1997) J Am Chem Soc 119:11395–11400
48. Harris TV, Szilagyi RK (2011) Inorg Chem 50:4811–4824
49. Bjornsson R, Lima FA, Spatzal T, Weyhermueller T, Glatzel P, Einsle O, Neese F, DeBeer S (2014) Chem Sci 5:3096–3103
50. Cramer SP, Gillum WO, Hodgson KO, Mortenson LE, Stiefel EI, Chisnell JR, Brill WJ, Shah VK (1978) J Am Chem Soc 100:3814–3819
51. Hoffman BM, Roberts JE, Orme-Johnson WH (1982) J Am Chem Soc 104:860–862
52. Venters RA, Nelson MJ, McLean PA, True AE, Levy MA, Hoffman BM, Orme-Johnson WH (1986) J Am Chem Soc 108:3487–3498
53. True AE, McLean P, Nelson MJ, Orme-Johnson WH, Hoffman BM (1990) J Am Chem Soc 112:651–657
54. Hedman B, Frank P, Gheller SF, Roe AL, Newton WE, Hodgson KO (1988) J Am Chem Soc 110:3798–3805
55. Lovell T, Torres RA, Han W, Liu T, Case DA, Noodleman L (2002) Inorg Chem 41:5744–5753
56. Lovell TT, Liu TT, Case DA, Noodleman L (2003) J Am Chem Soc 125:8377–8383
57. Lukoyanov D, Pelmenschikov V, Maeser N, Laryukhin M, Yang TC, Noodleman L, Dean DR, Case DA, Seefeldt LC, Hoffman BM (2007) Inorg Chem 46:11437–11449
58. Dance I (2011) Inorg Chem 50:178–192
59. Armstrong WH, Mascharak PK, Holm RH (1982) Inorg Chem 21:1699–1701
60. Mascharak PK, Papaefthymiou GC, Armstrong WH, Foner S, Frankel RB, Holm RH (1983) Inorg Chem 22:2851–2858
61. Mizobe Y, Mascharak PK, Palermo RE, Holm RH (1983) Inorg Chim Acta 80:L65–L67
62. Zhang Y, Holm RH (2003) J Am Chem Soc 125:3910–3920
63. Liu Q, Huang L, Liu H, Lei X, Wu D, Kang B, Lu J (1990) Inorg Chem 29:4131–4137
64. Coucouvanis D, Al-Ahmad S, Salifoglou A, Dunham WR, Sands RH (1988) Angew Chem Int Ed 27:1353–1355
65. Coucouvanis D, Al-Ahmad SA, Salifoglou A, Papaefthymiou V, Kostikas A, Simopoulos A (1992) J Am Chem Soc 114:2472–2482
66. Raebiger JW, Crawford CA, Zhou J, Holm RH (1997) Inorg Chem 36:994–1003
67. Carney MJ, Kovacs JA, Zhang YP, Papaefthymiou GC, Spartalian K, Frankel RB, Holm RH (1987) Inorg Chem 26:719–724
68. Hauser C, Bill E, Holm RH (2002) Inorg Chem 41:1615–1624
69. Arber JM, Dobson BR, Eady RR, Stevens P, Hasnain SS, Garner CD, Smith BE (1987) Nature 325:372–374
70. Cook M, Karplus M (1985) J Am Chem Soc 107:257–259
71. Cook M, Karplus M (1985) J Chem Phys 83:6344
72. Glatzel P, Smolentsev G, Bunker G (2009) J Phys Conf Ser 190:012046
73. Kurashige Y, Chan GK, Yanai T (2013) Nat Chem 5:660–666
74. Sharma S, Sivalingam K, Neese F, Chan GKL (2014) Nat Chem 6:927–933
75. Bjornsson R, Delgado-Jaime MU, Lima FA, Sippel D, Schlesier J, Weyhermüller T, Einsle O, Neese F, DeBeer S (2015) Z Anorg Allg Chem. doi:10.1002/zaac.201400446
76. Hoffman BM, Lukoyanov D, Dean DR, Seefeldt LC (2013) Acc Chem Res 46:587–595
77. Hoffman BM, Lukoyanov D, Yang ZY, Dean DR, Seefeldt LC (2014) Chem Rev 114:4041–4062
78. Christou G, Hageman RV, Holm RH (1980) J Am Chem Soc 102:7600–7601
79. Yamamura T, Christou G, Holm RH (1983) Inorg Chem 22:939–949
80. Smith BE, Durrant MC, Fairhurst SA, Gormal CA, Grönberg KLC, Henderson RA, Ibrahim SK, Le Gall T, Pickett CJ (1999) Coord Chem Rev 185:669–687
81. Gall TL, Ibrahim SK, Gormal CA, Smith BE, Pickett CJ (1999) Chem Commun 9:773–774
82. Pickett CJ, Vincent KA, Ibrahim SK, Gormal CA, Smith BE, Best SP (2003) Chem Eur J 9:76–87
83. Yuhas BD, Smeigh AL, Douvalis AP, Wasielewski MR, Kanatzidis MG (2012) J Am Chem Soc 134:10353–10356
84. Coucouvanis D, Demadis KD, Malinak SM, Mosier PE, Tyson MA, Laughlin LJ (1996) J Mol Catal A Chem 107:123–135
85. Coucouvanis D, Demadis KD, Malinak SM, Mosier PE, Tyson MA, Laughlin LJ (1996) Transition metal sulfur chemistry. ACS Symp Ser 653:117–134
86. Malinak SM, Demadis KD, Coucouvanis D (1995) J Am Chem Soc 117:3126–3133
87. Coucouvanis D, Mosier PE, Demadis KD, Patton S, Malinak SM, Kim CG, Tyson MA (1993) J Am Chem Soc 115:12193–12194
88. Demadis KD, Malinak SM, Coucouvanis D (1996) Inorg Chem 35:4038–4046
89. Laughlin LJ, Coucouvanis D (1995) J Am Chem Soc 117:3118–3125

90. Malinak SM, Simeonov AM, Mosier PE, McKenna CE, Coucouvanis D (1997) J Am Chem Soc 119:1662–1667
91. Hoover TR, Imperial J, Liang J, Ludden PW, Shah VK (1988) Biochemistry 27:3647–3652
92. Imperial J, Hoover TR, Madden MS, Ludden PW, Shah VK (1989) Biochemistry 28:7796–7799
93. Coucouvanis D (1996) JBIC 1:594–600
94. Allen AD, Senoff CV (1965) Chem Commun(London) 24:621–622
95. Fryzuk MD, Johnson SA (2000) Coord Chem Rev 200:379–409
96. Hidai M, Mizobe Y (1995) Chem Rev 95:1115–1133
97. Hidai M (1999) Coord Chem Rev 185:99–108
98. Chatt J, Dilworth JR, Richards RL (1978) Chem Rev 78:589–625
99. Richards RL (1996) Coord Chem Rev 154:83–97
100. Richards RL (1996) Pure Appl Chem 68:1521–1526
101. Bazhenova TA, Shilov AE (1995) Coord Chem Rev 144:69–145
102. Yandulov DV, Schrock RR (2003) Science 301:76–78
103. Schrock RR (2005) Acc Chem Res 38:955–962
104. Schrock RR (2008) Angew Chem Int Ed 47:5512–5522
105. Yandulov DV, Schrock RR (2005) Inorg Chem 44:1103–1117
106. McNaughton RL, Roemelt M, Chin JM, Schrock RR, Neese F, Hoffman BM (2010) J Am Chem Soc 132:8645–8656
107. Studt F, Tuczek F (2005) Angew Chem Int Ed 44:5639–5642
108. Munisamy T, Schrock RR (2012) Dalton Trans 41:130–137
109. Schenk S, Le Guennic B, Kirchner B, Reiher M (2008) Inorg Chem 47:3634–3650
110. Arashiba K, Miyake Y, Nishibayashi Y (2010) Nat Chem 3:120–125
111. Anderson JS, Rittle J, Peters JC (2013) Nature 501:84–87
112. Creutz SE, Peters JC (2014) J Am Chem Soc 136:1105–1115
113. Rittle J, Peters JC (2013) Proc Natl Acad Sci USA 110:15898–15903
114. MacLeod KC, Holland PL (2013) Nat Chem 5:559–565
115. Barney BM, Igarashi RY, Dos Santos PC, Dean DR, Seefeldt LC (2004) J Biol Chem 279:53621–53624
116. Sarma R, Barney BM, Keable S, Dean DR, Seefeldt LC, Peters JW (2010) J Inorg Biochem 104:385–389